JUNE 21 2019

# Active cancellation of sound generated by finite length coherent line sources using piston-like secondary source arrays

Qi Hu; S. K. Tang



*J. Acoust. Soc. Am.* 145, 3647–3655 (2019)
https://doi.org/10.1121/1.5112761

# Active cancellation of sound generated by finite length coherent line sources using piston-like secondary source arrays

Qi Hu and S. K. Tang[a)]
*Department of Building Services Engineering, The Hong Kong Polytechnic University, Hong Kong, China*

(Received 28 January 2019; revised 21 May 2019; accepted 2 June 2019; published online 21 June 2019)

The active cancellation of the sound generated by finite length coherent line sources is investigated numerically in the present study. A secondary source consists of a central circular core enclosed within an annulus is proposed. It is demonstrated that this source type can produce a much more directional secondary sound field than a single circular piston, even its size is much smaller than the latter if its two parts are vibrating out-of-phase with the right magnitude ratio. This property gives rise to more effective spanwise sound reduction. An example of a secondary source array for broadband noise control is also provided. Though the control performance becomes weaker as frequency increases, the noise reduction within the central region of the receiver plane remains significant in all the cases included in the present study. © *2019 Acoustical Society of America*.
https://doi.org/10.1121/1.5112761

[KVH] Pages: 3647–3655

## I. INTRODUCTION

Noise control, be it in the indoor and outdoor, is always an important issue in compact cities as excessive exposure to noise is hazardous to human health.[1] It is also understood that prolonged exposure to noise even at levels well below statutory control levels is problematic.[2] There is a recent report from WHO[3] warning that noise has become the second environmental pollution leading to human death in western Europe. Though there is no similar study in other parts of the world, it is believed that the problem is not just European.

There have been many passive and active mitigation methods proposed in the past few decades to help alleviate this worldwide problem. There are many daily life examples of passive methods. The massive roadside noise barrier[4] is a typical example applied in the outdoors. In the indoors, dissipative silencers and sound absorption panels are commonly used.[5] The plenum window design of Tong *et al.*[6] is also a passive noise reduction device, but it can allow for a reasonable level of natural ventilation inside the associated residential flats.

Active control, where a secondary sound system is used to cancel an unwanted sound,[7] is less popular though it has been proven workable in the confined air conditioning and ventilation ductwork.[8] In the indoors, complete global reduction of noise by active mean is basically not possible and thus, the creation of quiet zones is the focus.[9,10] When the primary source is confined such that the propagation of noise from the source to the receivers is basically understood, active control using multiple secondary sources and error sensors is effective.[11] Active control can also be combined with passive methods for improved performance. Examples of these works include the active noise barrier edges of Omoto and Fujiwara[12] and Hart and Lau,[13] the active window edges of Kwon and Park[14] and the investigation of active control effectiveness inside plenum windows of Huang *et al.*[15] and Tong *et al.*[16]

Standalone active environmental noise control system, which is not attached to a passive device, for cancelling noise in the free field is not commonly found in existing literature. Wright and Vuksanovic[17,18] have developed a theory to investigate the active control of non-compact primary noise source using a monopole secondary source array. They observed excellent noise cancellation at specific locations, but sound amplification could be serious at some other locations. Guo *et al.*[19] studied the creation of quiet zone in the free field by a control source array. Duhamel and Sergent[20] described a formulation for attenuating actively an incoherent line source. There are also efforts studying the use of multipoles to cancel the sound from a compact primary source (for instance, Bolton *et al.*[21] and Chen *et al.*[22]).

Noise barriers in the countryside or suburban areas are not so welcomed by the residents as they tend to obstruct views. In the indoors, there are noises from linear air grilles or similar non-compact structures in the building occupied zones which cannot be screened because of air distribution and air flow performance issues.[23] The virtual barrier idea of Tao *et al.*[11] is, therefore, an interesting option for noise control. In this study, an attempt is made to attenuate noise from a finite length coherent line source in free field using an array of directional secondary sources of reasonably small size to create a virtual noise barrier. The effective control zones will be examined in detail.

## II. ACTIVE CONTROL FORMULATION

The formulation of the active control is based on that of Wright and Vuksanovic.[18] Figure 1 illustrates the setup of the present system, which consists of a coherent line source of length $l$, error microphones on the vertical monitoring plane $S_{mp}$, and secondary sources located in parallel with the primary source. For simplicity, the number of secondary

a)Electronic mail: shiu-keung.tang@polyu.edu.hk

sources is set equal to that of the error sensors. The origin of the system is set at the centre of the line source. The monitoring plane is at $x = d_{mp}$ and the secondary sources at $x = d_{ss}$. The separation between adjacent secondary sources is $d_s$ and that between adjacent error microphones $d_e$. The system is symmetric about the axis $y = 0$. The performance of the active control is described by the sound pressure level reduction on the monitoring plane, which measures $l_{mp}$ in length by $h_{mp}$ in height. All the sound sources are fixed on the horizontal $xy$-plane.

The sound created by a finite length coherent line source at any point $\mathbf{x} = (x, y, z)$ in the far field is[24]

$$p(\mathbf{x}) = j\frac{\rho ck}{4\pi}\frac{\sin\left(\frac{kl}{2}\sin\theta\right)}{\frac{kl}{2}\sin\theta}\frac{Q_l}{r}e^{-jkr}, \tag{1}$$

where $k$ is the wavenumber, $c$ the ambient speed of sound, $\rho$ the density of the medium, $Q_l$ the strength of the line source, $j = \sqrt{-1}$, $r = \sqrt{x^2 + y^2 + z^2}$, and $\sin\theta = y/r$. When $y/r \to 0$, the factor $\sin(kl\sin\theta/2)/(kl\sin\theta/2) \to 1$. The sound pressure created by an axisymmetric compact secondary source located at $\mathbf{x}_s = (x_s, y_s, 0)$ at $\mathbf{x}$ is, for $|\mathbf{x} - \mathbf{x}_s| \gg$ source radius:

$$p_s(\mathbf{x}) = j\frac{\rho ck}{4\pi}D_s(|\mathbf{x} - \mathbf{x}_s|, \varphi)\frac{Q_s}{|\mathbf{x} - \mathbf{x}_s|}e^{-jk|\mathbf{x}-\mathbf{x}_s|}, \tag{2}$$

where $Q_s$ is the complex source strength and $D_s$ the directivity factor which is, in general, a function of the distance $|\mathbf{x} - \mathbf{x}_s|$ and the angle between the vector $\mathbf{x} - \mathbf{x}_s$ and the surface normal of the source, $\varphi$. For a monopole source, $D_s = 1$. Suppose there are $N$ number of secondary sources and thus $N$ number of error microphones, the sound pressure at the $i$th error microphone at $\mathbf{x}_{ei} = (x_{ei}, y_{ei}, z_{ei})$ is

$$p_{ei} = p(\mathbf{x}_{ei}) + \sum_{n=1}^{N} p_{sn}(\mathbf{x}_{ei}). \tag{3}$$

The target is to optimize the secondary source strength vector $\mathbf{Q}_s = [Q_{s1}, Q_{s2}, Q_{s3}, \ldots, Q_{sN}]$ such that the total potential energy[25] at the error microphones $\mathbf{p}_e^H\mathbf{p}_e$ is at its minimum, where $\mathbf{p}_e = [p_{e1}, p_{e2}, p_{e3}, \ldots, p_{eN}]$ and $H$ denotes the Hermitian transpose. The optimized $\mathbf{Q}_{s,opt}$ is

$$\mathbf{Q}_{s,opt} = -\mathbf{Z}_s^{-1}\mathbf{Z}_p Q_l, \tag{4}$$

where $\mathbf{Z}_p$ is a $N \times 1$ matrix with its $i$th element represented by

$$\mathbf{Z}_p(i) = j\frac{\rho ck}{4\pi}\frac{\sin\left(\frac{kl}{2}\sin\theta_i\right)}{\frac{kl}{2}\sin\theta_i}\frac{e^{-jk|\mathbf{x}_{ei}|}}{|\mathbf{x}_{ei}|} \tag{5a}$$

and $\mathbf{Z}_s$ is a $N \times N$ matrix with

$$\mathbf{Z}_s(i,n) = j\frac{\rho ck}{4\pi}D_s(|\mathbf{x}_{ei} - \mathbf{x}_{sn}|, \varphi_{in})\frac{e^{-jk|\mathbf{x}_{ei}-\mathbf{x}_{sn}|}}{2|\mathbf{x}_{ei} - \mathbf{x}_{sn}|}. \tag{5b}$$

Details of the optimization process can be found in Refs. 16 and 20 and thus are not repeated here. With all the above information, the sound pressure level at any point on the vertical monitoring plane can be calculated. Apart from the distribution of sound pressure on this monitoring plane, the reduction of the average sound pressure level on this plane will also be used as a descriptor of the active control performance.

## III. ACTIVE CONTROL WITH SIMPLE SECONDRY SOURCES

For illustration purposes, $d_{mp}$, $d_{ss}$, and $l$ are set at 100, 1, and 10 m, respectively, in the foregoing analysis unless otherwise specified. The span of the monitoring plane is fixed with $l_{mp} = 500$ m and $h_{mp} = 50$ m. A long horizontal span length is chosen here in order to understand the effective spatial range of the active control. The simplest secondary sources are the monopoles and circular pistons.

For monopoles, $D_s = 1$ and for a compact circular piston of radius $r_o$,[24]

$$D_s = \frac{4J_1(kr_o\sin\varphi)}{kr_o\sin\varphi}, \tag{6}$$

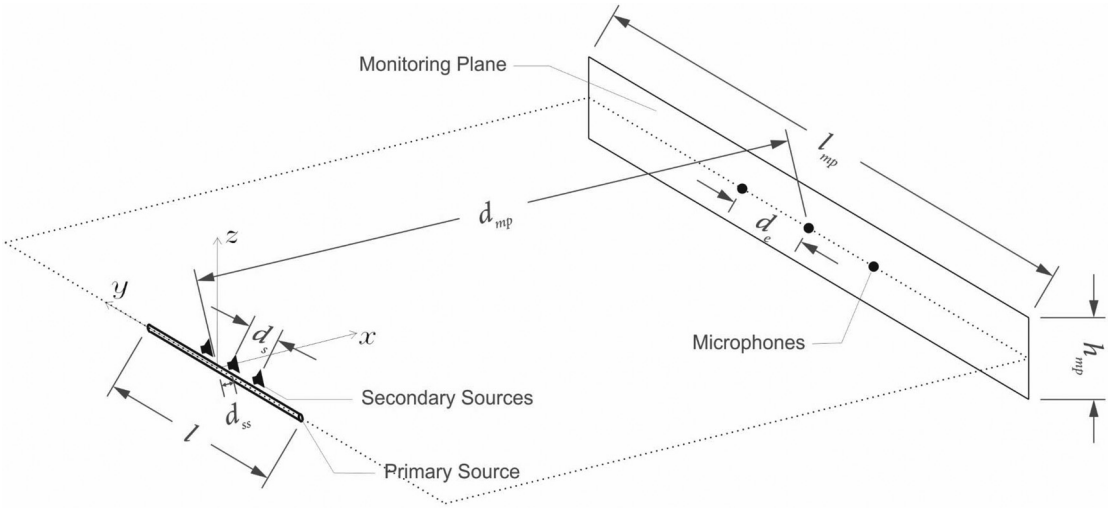


FIG. 1. Schematics of the present active control setting and the nomenclature adopted.

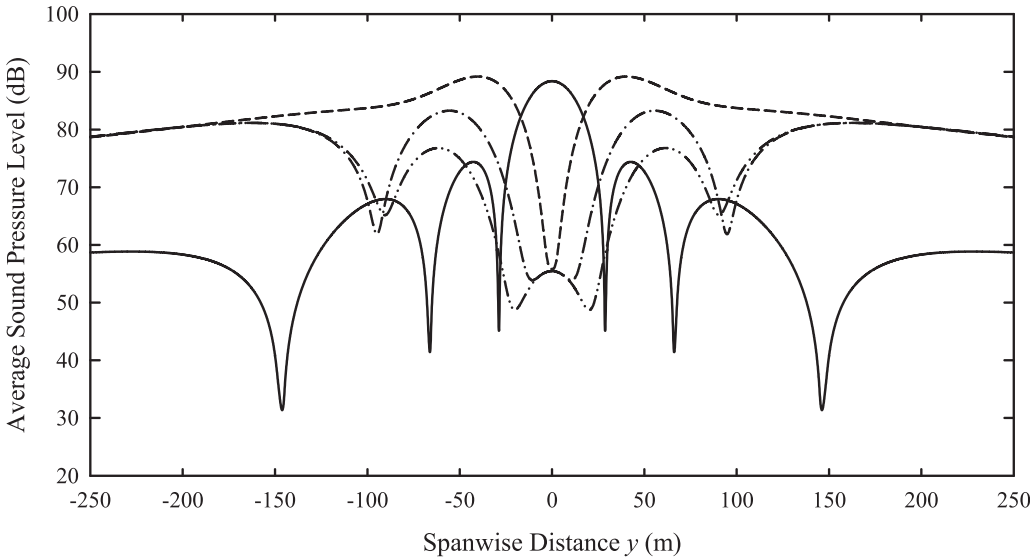


FIG. 2. Spanwise variation of average sound pressure level on the monitoring plane at the low frequency of 125 Hz with piston control sources of radius $r_o = 0.5$ m. ———: No active control; – – – –: number of control source $N = 1$; — · —: $N = 3$; — ·· —: $N = 5$.

where $J_1$ is the Bessel function of the first kind. Figure 2 shows the spanwise variation of average sound pressure level on the monitoring plane at the frequency of 125 Hz with a different number of secondary sources with $r_o = 0.5$ m. Though a secondary source of radius 0.5 m is not so practical, it is used here for illustration purpose. As the sound pressure level variation with height on the monitoring plane is small, the data presented in Fig. 2 are those logarithmically averaged along the height ($z$-direction). It can be observed that the effectiveness of the active control is very good at locations near to the central plane of the system. However, there is considerable sound amplification at the region $|y| > 2l$ on the monitoring plane. Similar observations have been made by Wright and Vuksanovic.[17] For the case of a single secondary source with a single error microphone located on the centerline of the system, the resultant sound has a magnitude even higher than the maximum sound level in the "no control" case due to the constructive interface between the secondary source and the primary noise source. The attenuation zone becomes larger and the amplitude of the resultant sound field is lowered as $N$ increases, but such effect is not obvious at the far-away monitoring points. It is found that the circular piston gives only slightly better performance than the monopoles at this frequency. The results of the monopole control are thus not presented.

Figure 3 shows the performance of the active control when the sound frequency is increased to 500 Hz with $N$ fixed at 5. One can observe that the control is always effective on the central plane of the monitoring plane. However, the performance of the active control becomes worse as $r_o$ decreases. A smaller piston diameter results in less directional sound radiation as shown in Fig. 4. Though the effectiveness of the active control depends also on the characteristics of the primary sound source,[26] the results shown in Figs. 3 and 4 tend to

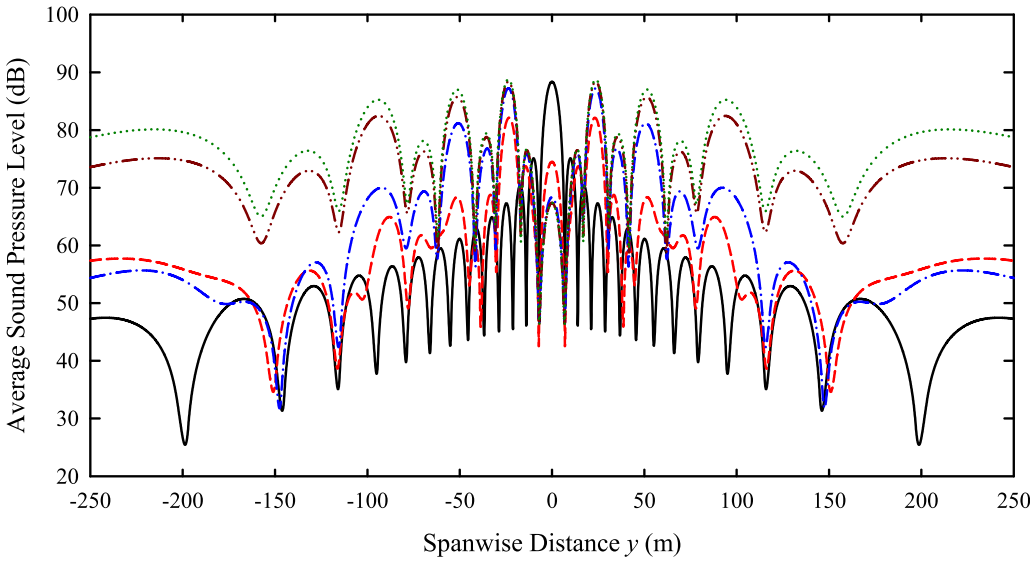


FIG. 3. (Color online) Spanwise variation of average sound pressure level on the monitoring plane obtained using piston control sources of different radius $r_o$ at the frequency of 500 Hz. Number of sources $N = 5$, control source separation $d_s$ = error microphone separation $d_e = 3$ m. ———: No active control; – – – –: $r_o = 1$ m; — · —: $r_o = 0.5$ m; — ·· —: $r_o = 0.25$ m; · · · · · ·: $r_o = 0.05$ m.

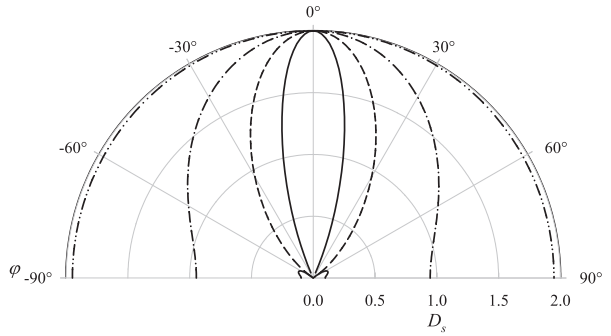


FIG. 4. Effect of control source radius $r_o$ on the directivity pattern of piston radiation at the frequency of 500 Hz. ———: $r_o = 1$ m; – – – –: $r_o = 0.5$ m; — · —: $r_o = 0.25$ m; — ·· —: $r_o = 0.05$ m.

suggest that a less directional secondary source could lower the overall performance of the present active control system. However, a smaller secondary source can allow more such sources to be used within a fixed spatial span for the enhancement of active control performance. The main objective of this study is to derive a reasonably compact secondary control source system which can achieve broadband active reduction of sound generated by a finite length coherent line source.

## IV. THE NEW SECONDARY SOURCE AND ITS PERFORMANCE

A new secondary source consists of an outer annulus of outer radius $r_o$ and an inner circular piston core of radius $r_i$ as shown in Fig. 5 is proposed in this section. Its directivity can be controlled by adjusting the phase difference between as well as the magnitudes of the two vibrating components. Apart from its directivity, its size is also a major concern and the effect of source radius on the effectiveness of the active control will be examined.

The sound pressure at a point $\mathbf{x}$ due to this source is

$$p = j\frac{\rho ckQ}{\pi}\frac{e^{-jk|\mathbf{x}-\mathbf{x}_s|}}{|\mathbf{x}-\mathbf{x}_s|}\left[\frac{J_1(kr_i\sin\varphi)}{kr_i\sin\varphi} + e^{j\phi}R_v \times \left(R_r^2\frac{J_1(kr_o\sin\varphi)}{kr_o\sin\varphi} - \frac{J_1(kr_i\sin\varphi)}{kr_i\sin\varphi}\right)\right], \quad (7)$$

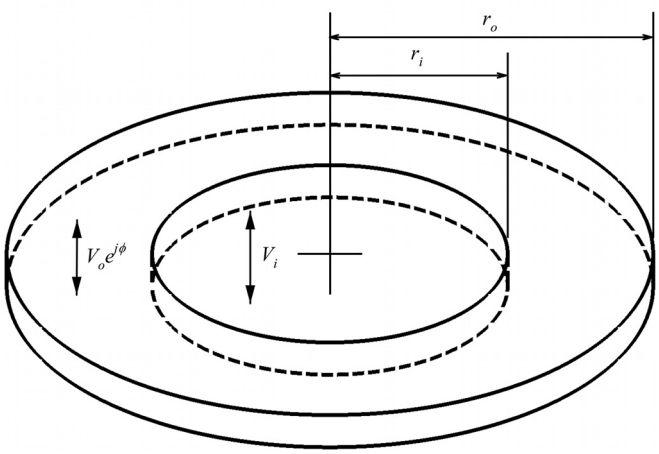


FIG. 5. The newly proposed secondary source.

where $\phi$ is the phase difference between the two vibrating surfaces, $Q = \pi r_i^2 V_i$ ($V$ is the vibrating velocity), $R_v = V_o/V_i$, $R_r = r_o/r_i$, and the suffices $o$ and $i$ represent the quantity associated with the outer annulus and inner core, respectively. It can be inferred from Eq. (7) that the sound field generated by this concentric piston source can be set more directional than that of a single piston of the same $r_o$ at the same frequency.

The directivity $D$ of an axisymmetric source can be defined using the formula:[24]

$$D = 2\left(\int_0^{\pi/2} H^2(\varphi)\sin\varphi d\varphi\right)^{-1}, \quad (8)$$

where $H$ is referred to as the directional factor and $H = p(|\mathbf{x}-\mathbf{x}_s|,\varphi)/p(|\mathbf{x}-\mathbf{x}_s|,0)$. It is straightforward to show that the magnitude of $D$ is the largest when $\phi = \pi$ for a fixed pair of $R_v$ and $R_r$. In the rest of the discussions, $\phi$ is set equal to $\pi$. The two components of the newly proposed secondary source are vibrating out-of-phase.

Figure 6(a) illustrates the effects of $R_v$ and $R_r$ on $D$ at the frequency of 500 Hz for $r_o = 0.05$ m. It can be observed

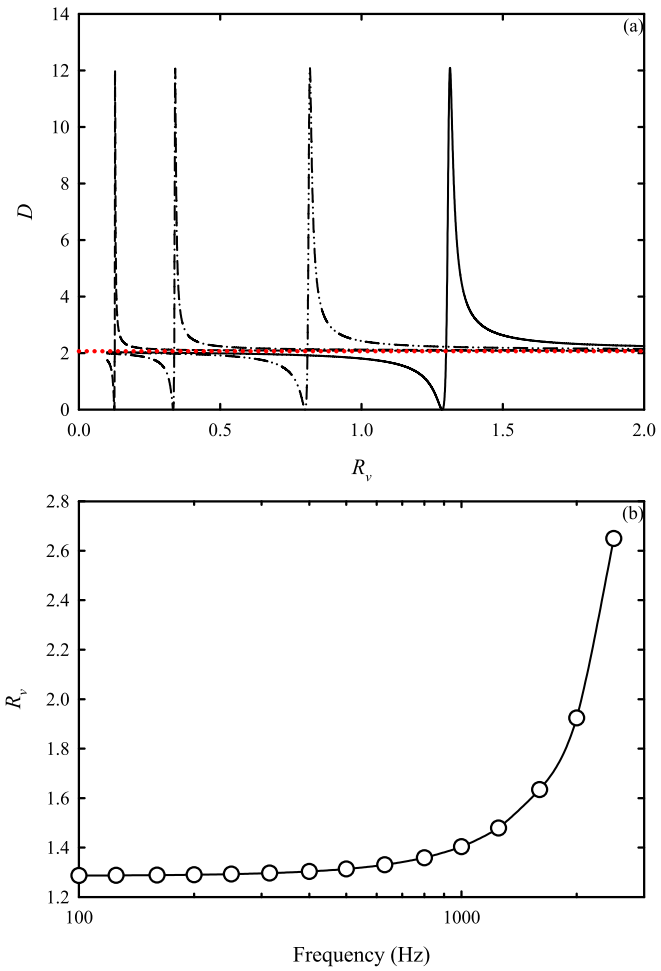


FIG. 6. (Color online) (a) Effects of velocity ratio $R_v$ and radius ratio $R_r$ on source directivity $D$ at the frequency of 500 Hz. Control source radius $r_o = 0.05$m. ———: $R_r = 4/3$; — ·· —: $R_r = 3/2$; — · —: $R_r = 2$; – – – –: $R_r = 3$;· · · · · ·: piston. (b) Variation of velocity ratio $R_v$ with frequency for $R_r = 4/3$ and $r_o = 0.05$ m.

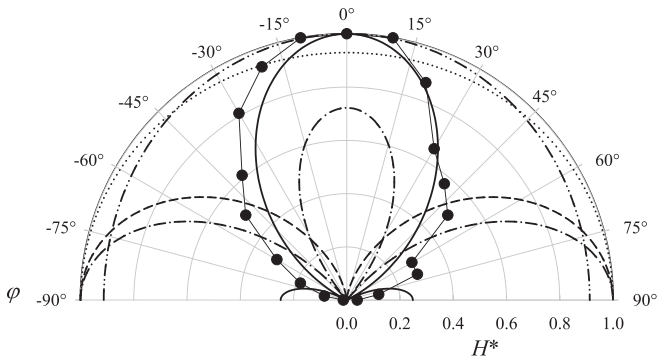


FIG. 7. Variation of directional sound radiation patterns of the newly proposed source with velocity ratio $R_v$ at the frequency of 500 Hz. Control source radius $r_o = 0.05$ m. · · · · · ·: $R_v = 1$; – – – –: $R_v = 1.2857$ (minimum directivity); — · —: $R_v = 1.2999$; ———: $R_v = 1.3132$ (maximum directivity); — ·· —: $R_v = 2$. — • —: Compound source of Chen *et al.* (Ref. 22).

that the new source can produce a very directional sound field with $D > 10$ under suitable combinations of $R_v$ and $R_r$. There are cases where $D = 0$, which represent the situation at which no resultant sound is radiated out along the axis $\varphi = 0$. The $R_v$ resulted in the largest $D$ increases with decreasing $R_r$. The $D$ of a simple circular piston is also presented in Fig. 6(a) for the sake of easy comparison. One can observe that the newly proposed secondary source can produce much more directional sound field than a single circular piston, even when the size of the new source is much smaller than that of the piston. A similar phenomenon is also observed at higher frequencies and thus the corresponding results are not presented. The $R_v$ resulted in maximum $D$ increases with frequency for a fixed $R_r$ as shown in Fig. 6(b). The rate of increase is very slow at a frequency below 1000 Hz, but it becomes relatively rapid afterward.

Figure 7 illustrates the effect of $R_v$ on the variation of sound radiation pattern $H^*$ generated by the newly proposed source with $R_r = 4/3$ and $r_o = 0.05$ m at 500 Hz. $H^*$ is the sound magnitude $p(|\mathbf{x} - \mathbf{x}_s|, \varphi)$ normalized by the corresponding strongest sound radiation magnitude. At $R_v = 1$ and 2, the radiation is monopole-like and the direction of stronger sound radiation is at $\varphi = \pm 90°$ and $\varphi = 0°$, respectively. At minimum $D$ ($D \sim 0$), the lateral sound radiation is very strong, leaving the frontal radiation insignificant (or even no frontal radiation). As $R_v$ increases, a gradual increase in the frontal sound radiation strength is observed. However, the lateral and frontal sound radiation is 180° out-of-phase (not shown here). At $R_v = 1.3132$, where maximum $D$ is recorded, the radiation is extremely frontal. Comparing to the results of piston source (Fig. 4) and that of the compound source of Chen *et al.*,[22] the newly proposed source can produce more directional sound radiation even if its diameter is small. The newly proposed source also gives a directivity much stronger that those of the multipoles of Beauvilain *et al.*[27] at 250 Hz (not shown here). Basically, similar pattern of $D$ variation with $R_v$ can be observed at other frequencies and thus the corresponding results are not presented.

The active sound cancellation performance resulted from using the new source with $R_r = 4/3$, $R_v = 1.3132$ is shown in Fig. 8 with $N$ kept at 5 and other system configurations the same as those in Fig. 3. This combination of $R_v$ and $R_r$ gives the most directional sound radiation at the tested frequency [Fig. 6(a)]. It is noticed by comparing the results shown in Figs. 3 and 8 that the spatial span of effective active attenuation is very much enlarged by using the newly proposed secondary source. The magnitude of the resultant sound field is also significantly lower than that resulted from the single piston secondary source cases. It should be noted that smaller overall size of the new source enables the adoption of more secondary sources in the active control system, though the system will become more complicated afterward. The foregoing discussions will be focused on the effects of $d_s$ and $d_e$ on the performance of the active control implemented using the new secondary source for different $N$. Without loss of generality, $R_r$ is set at 4/3 with $r_o = 0.05$ m.

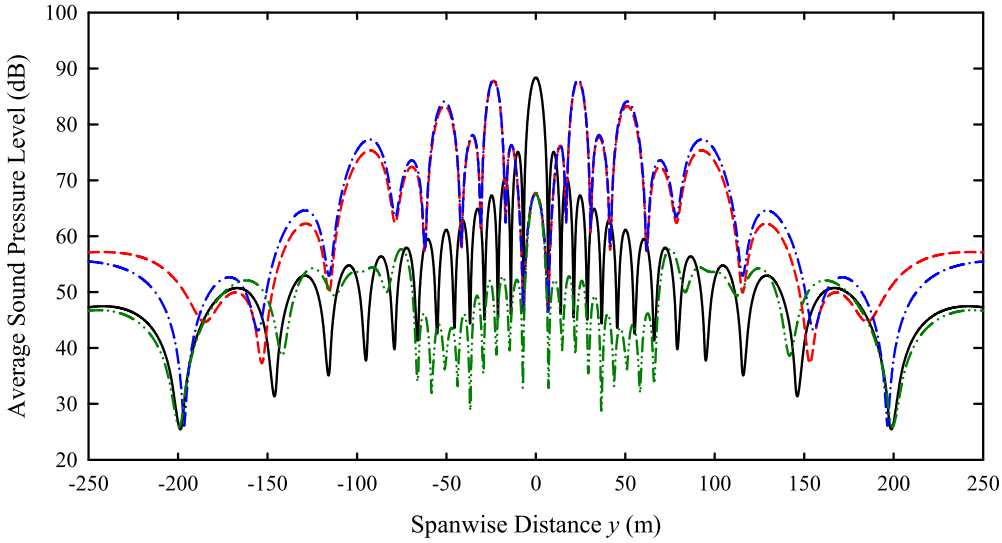


FIG. 8. (Color online) Spanwise variation of average sound pressure level on the monitoring plane obtained using the new secondary sources (radius ratio $R_r = 4/3$, velocity ratio $R_v = 1.3132$) at the frequency of 500 Hz. ———: No active control; $N = 5$, $d_s = d_e = 3$ m: – – – –: $r_o = 0.05$ m; — · —: $r_o = 0.25$ m. $N = 19$, $d_s = 0.6$ m, $d_e = 7.3$ m (Optimized setting): — ·· —: $r_o = 0.05$ m.

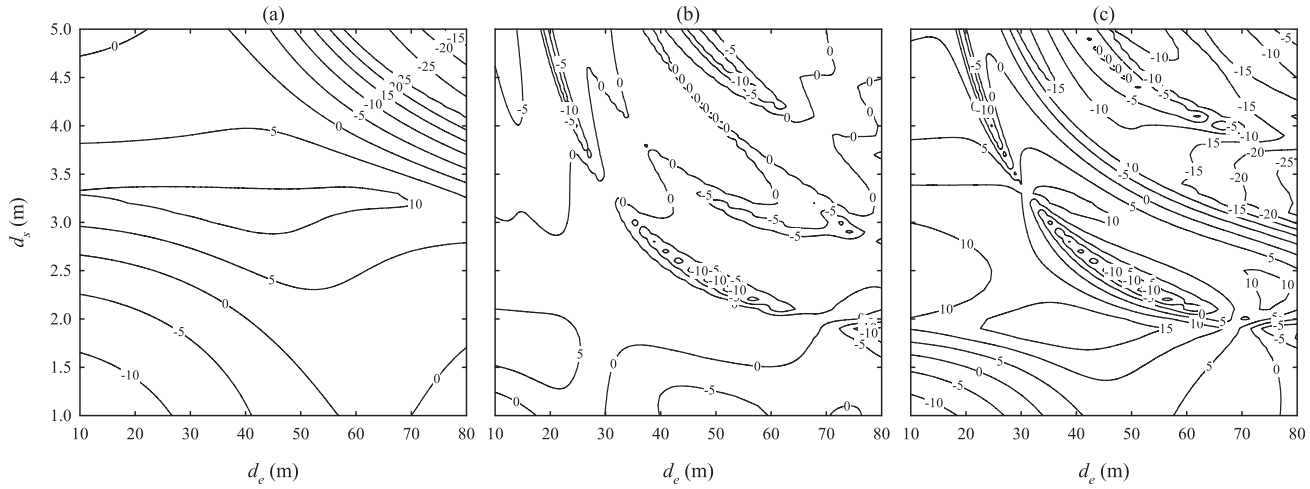


FIG. 9. Variations of total potential energy reduction Δ with number of control sources $N$, control source separation $d_s$ and error microphone separation $d_e$ at the frequency of 125 Hz. $r_o = 0.05$ m, $R_r = 4/3$, $R_v = 1.2874$. (a) $N = 3$; (b) $N = 4$; (c) $N = 5$.

The total potential energy reduction on the monitoring plane $S_{mp}$, Δ is used as the descriptor of the active control effectiveness:

$$\Delta = -10\log_{10}\left(\iint_{S_{mp}}\left|p + \sum_{n=1}^{N} p_{sn}\right|^2 dydz \Big/ \iint_{S_{mp}}|p|^2 dydz\right). \tag{9}$$

In the surface integration, $S_{mp}$ is discretized into regular grids with dimensions $dy$ and $dz$ set according to the frequency of interest and for simplicity, $dy = dz$. It should be noted that while $d_s$ is restricted by the length of the linear source and the size of the secondary source, $d_e$ can vary over a larger range for noise control effectiveness.

The combination of $d_s$ and $d_e$ significantly affects the noise control effectiveness Δ at a fixed frequency and $N$ as shown in Fig. 9. There is an optimal combination of $d_s$ and $d_e$ at which the largest Δ is obtained for a fixed $N$. It is also observed that the secondary source array with odd number of sources performs better than its even number counterpart [e.g., Fig. 9(b)]. Besides, it appears that a larger $N$ will result in larger optimal Δ (discussed further later in the paper). The same phenomenon is observed at other frequencies. The rest of the paper is focused on the development of new secondary source arrays for broadband application. Therefore, only the odd $N$ cases with microphones and secondary sources arranged symmetrically about the central plane ($y = 0$ m) will be considered.

Figure 10 shows the variations of $d_s$, $d_e$, and Δ with $N$ at the frequency of 1000 Hz. It is observed that Δ does not vary much or the rate of increase of Δ is very slow when $N$ exceeds a certain level. The same phenomenon is also observed at other frequencies (not shown there). Some examples of the variations of $d_s$, $d_e$ as well as $N$ with frequency for optimal control are summarized in Table I. The optimal $N$ is chosen to be the number of secondary sources above which further improvement of Δ is less than 1 dB for $N < 100$ in this study. An example of the active control performance under optimized control setting at 500 Hz can be found in Fig. 8.

It is observed that the optimal $N$ increases while $d_s$ decreases with increasing frequency. Therefore, the smaller the size of the secondary source, the better the broadband control performance will be. One can also observe that the optimized Δ decreases with increasing frequency, which is quite typical for active control. However, the noise reduction within the region of $-50\,\text{m} < y < 50\,\text{m}$ is still strong at ~7.3 dB at 2500 Hz (not shown here) though the corresponding noise control effectiveness is not satisfactory. In addition, it is noticed that the product $(N-1)d_s$ does not vary much with frequency and is roughly equal to the length of the finite line source.

There is a cut-off frequency above which this kind of control system cannot perform well, though the noise cancellation on the central region ($-50$ m $< y < 50$ m) remains significant (not presented here). Under the current setup, this cut-off frequency is around 2700 Hz where Δ falls to ~0 dB. It should be noted that $d_s$ cannot be less than 0.1 m for a secondary source radius $r_o = 0.05$ m. However, one can expect

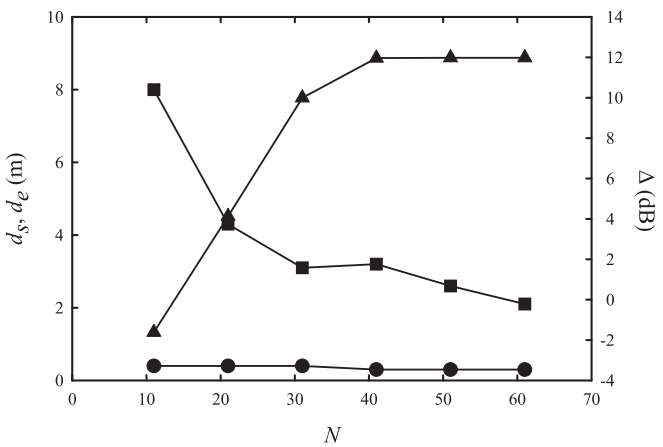


FIG. 10. Variations of $d_s$, $d_e$, and Δ with $N$ at the frequency of 1000 Hz. Control source radius $r_o = 0.05$ m, radius ratio $R_r = 4/3$, velocity ratio $R_v = 1.4031$. ●: $d_s$; ■: $d_e$; ▲: Δ.

TABLE I. Examples of optimal settings for control systems with the new secondary sources.

| Centre frequency (Hz) | Optimal control setting | | | |
|---|---|---|---|---|
| | Number of control source $N$ | Control source separation $d_s$ (m) | Error microphone separation $d_e$ (m) | Total potential energy reduction Δ (dB) |
| 125 | 7 | 1.9 | 29.8 | 20.4 |
| 250 | 13 | 0.9 | 15.7 | |
| 500 | 19 | 0.6 | 7.3 | 19.8 |
| 1000 | 35 | 0.3 | 3.7 | 16.2 |
| 2000 | 51 | 0.2 | 1.8 | 6.0 |
| 2500 | 51 | 0.2 | 1.4 | 2.2 |

the high frequency control performance of the present system will be improved if the size of the secondary source can be reduced further.

The bandwidth of effective active control varies with secondary source array setting and is relatively narrow except at low frequencies as shown in Fig. 11. Strong sound amplification is found outside the effective bandwidths. However, it is still possible to setup an assembly of secondary source arrays to provide significant broadband sound reduction, at least up to the cut-off frequency. Each array will look after the active control within a separate frequency band. One can actually start with the 250 Hz source array, which is already able to cover the active control at the frequencies between 65 to 280 Hz. Table II summarizes such an assembly and Fig. 12 illustrates the corresponding Δ spectrum. The spectral variation of Δ obtained within the central region $-50\,\text{m} < y < 50\,\text{m}$ using the secondary control source arrays given in Table II is also presented. Stronger noise reduction is observed within the central region.

It should be noted that the 25 arrays can be aligned into a single linear array assembly which is symmetrical about $y = 0$ as shown in Fig. 13 because of the small radii of the secondary sources. In this linear array assembly, a secondary source can be included in more than one individual array (A to Y). The actual number of secondary sources required is just 75. A large number of microphones is needed for the control, as expected.[25] One should also note that the number of secondary sources and error microphones can be reduced if one does not require optimal performance and/or high frequency noise attenuation. The latter is true for general traffic noise[28] and human noise control.[29]

The length of source, $l$, affects the active control performance. The number of secondary sources as well as that of error microphones required for optimal control performance

TABLE II. Secondary source array assembly for broadband active control.

| Array | Control band frequency (Hz) | | | Array setting | | |
|---|---|---|---|---|---|---|
| | Centre | Lower cut-off | Upper cut-off | $N$ | $d_s$ (m) | $d_e$ (m) |
| A | 250 | 65 | 280 | 13 | 0.9 | 15.7 |
| B | 350 | 280 | 370 | 13 | 0.9 | 10.8 |
| C | 400 | 370 | 430 | 19 | 0.6 | 9.6 |
| D | 500 | 430 | 525 | 19 | 0.6 | 7.3 |
| E | 600 | 525 | 635 | 19 | 0.6 | 5.8 |
| F | 680 | 635 | 730 | 29 | 0.4 | 5.1 |
| G | 800 | 730 | 845 | 29 | 0.4 | 4.2 |
| H | 900 | 845 | 970 | 29 | 0.4 | 3.6 |
| I | 1000 | 970 | 1060 | 35 | 0.3 | 3.7 |
| J | 1100 | 1060 | 1175 | 35 | 0.3 | 3.3 |
| K | 1250 | 1175 | 1300 | 35 | 0.3 | 2.9 |
| L | 1380 | 1300 | 1420 | 35 | 0.3 | 2.6 |
| M | 1450 | 1420 | 1475 | 57 | 0.2 | 2.4 |
| N | 1500 | 1475 | 1525 | 57 | 0.2 | 2.3 |
| O | 1550 | 1525 | 1585 | 57 | 0.2 | 2.2 |
| P | 1630 | 1585 | 1645 | 57 | 0.2 | 2.1 |
| Q | 1700 | 1645 | 1715 | 57 | 0.2 | 2.0 |
| R | 1750 | 1715 | 1790 | 57 | 0.2 | 1.9 |
| S | 1800 | 1790 | 1885 | 57 | 0.2 | 1.8 |
| T | 1900 | 1885 | 1970 | 51 | 0.2 | 1.9 |
| U | 2000 | 1970 | 2070 | 51 | 0.2 | 1.8 |
| V | 2100 | 2070 | 2180 | 51 | 0.2 | 1.7 |
| W | 2200 | 2180 | 2305 | 51 | 0.2 | 1.6 |
| X | 2400 | 2305 | 2445 | 51 | 0.2 | 1.5 |
| Y | 2500 | 2445 | 2605 | 51 | 0.2 | 1.4 |

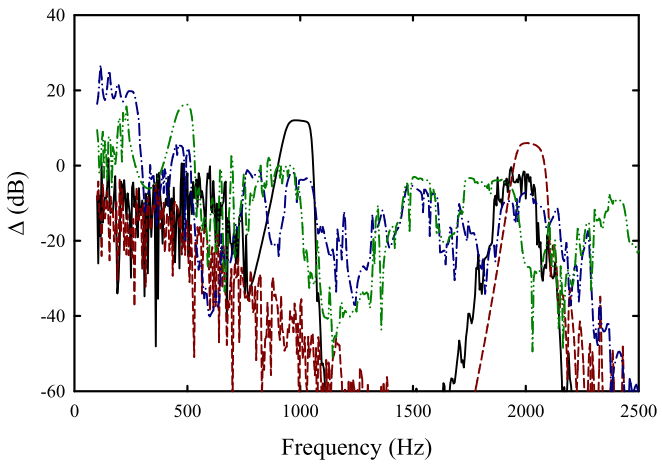


FIG. 11. (Color online) Examples of the spectral variations of total potential energy reduction Δ under optimal secondary source settings. — · —: 250 Hz; — ·· —: 500 Hz; ———: 1000 Hz; – – – –: 2000 Hz.

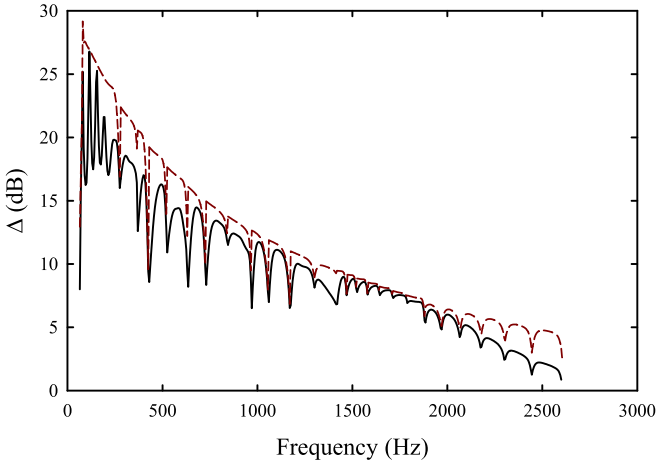


FIG. 12. (Color online) Spectrum of total potential energy reduction Δ obtained using the broadband active control assembly shown in Table II. ———: Δ within $-250\,\text{m} < y < 250\,\text{m}$; – – – –: Δ within $-50\,\text{m} < y < 50\,\text{m}$.

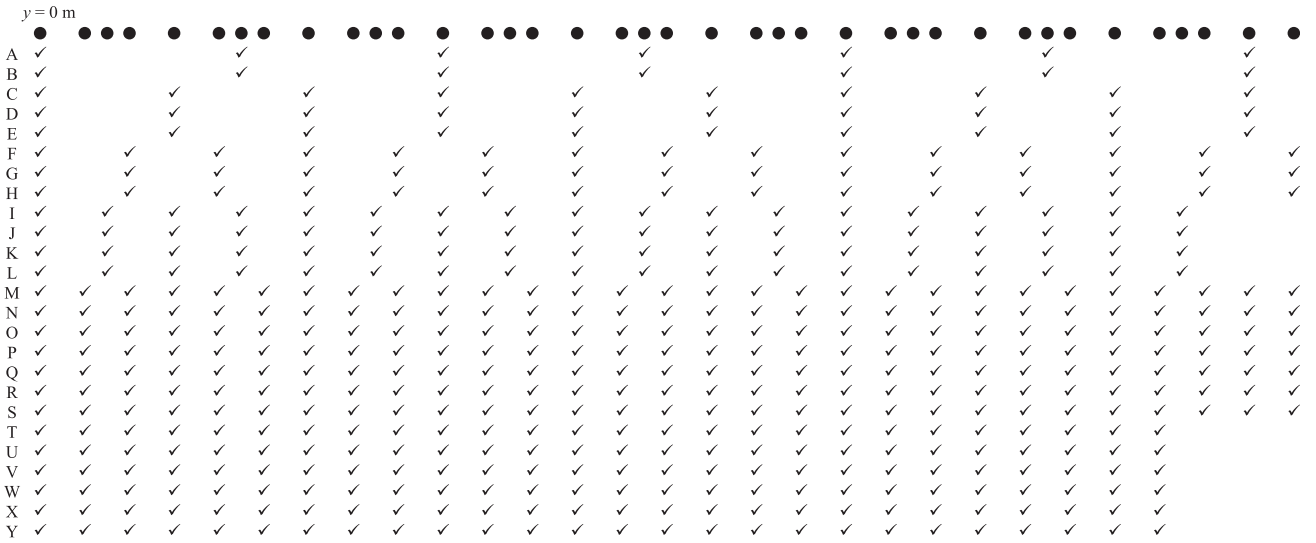


FIG. 13. Control source array arrangement for the assembly shown in Table II. ●: Secondary control source; ✓: control source included in an array (A to Y).

increase with the source length as expected. Since the corresponding results are basically in line with those of Guo *et al.*,[19] they are not discussed further.

## V. CONCLUSIONS

The active attenuation of noise radiated from a finite length coherent line source in an unbounded medium is studied numerically in the present investigation. A new secondary source consists of a central circular core and an outer annulus is proposed for the purpose. The working frequency range of the active control system is examined. In the present study, the effectiveness of active noise reduction is described by the reduction of the average sound pressure level on a 500 m long monitoring plane at a distance 100 m from the primary source. The frequency range of interest in this study is from 100 to 2500 Hz, which spans over the major frequency range of traffic noise and human speech.

It is found that the directivity of the secondary source is important for effective active control. The more directional the secondary sound field, the more effective the present active control will be. It is demonstrated that the newly proposed secondary source is able to produce a very directional sound field when its central core is vibrating out-of-phase with respect to the annulus at the right vibration magnitude ratio. Such directivity is much higher than those of a circular piston and some existing compound sources even the overall size of the new source is much smaller than the physical sizes of the other sources. This enables the use of more secondary sources within a relatively compact region, significantly improving the active control performance.

The numerical results confirm that the use of the new secondary sources gives rise to much improved active control systems than those can be achieved by pistons or monopoles. An example of broadband control is also given. Besides, it is found that the active control effectiveness can be improved by incorporating more secondary sources, but there exists a limit over which the use of more secondary sources does not result in significant improvement of control effectiveness. Moreover, the effectiveness of the active control system is found deteriorating with increasing frequency. However, the noise reduction within the central region of the monitoring plane, which has a span similar to the distance of the primary source from that plane, remains significant for all the cases investigated in this study.

## ACKNOWLEDGMENTS

Q.H. was supported by a studentship from the Research Committee, The Hong Kong Polytechnic University.

[1]K. D. Kryter, *The Effects of Noise on Man* (Academic, New York, 1985).
[2]J. Kang, K. Chourmouziadou, K. Sakantamis, B. Wang, and Y. Hao, *Soundscape of European Cities and Landscapes* (Soundscape-COST, Oxford, 2013).
[3]WHO, "Burden and disease from environmental noise," in *Quantification of Healthy Life Years Lost in Europe* (World Health Organization, Bonn, 2011).
[4]U. J. Kurze, "Noise reduction by barriers," J. Acoust. Soc. Am. **55**, 504–518 (1974).
[5]A. Fry, *Noise Control in Building Services* (Pergamon, New York, 1988).
[6]Y. G. Tong, S. K. Tang, J. Kang, A. Fung, and M. K. L. Yeung, "Full scale field study of sound transmission across plenum windows," Appl. Acoust. **89**, 244–253 (2015).
[7]P. A. Nelson and S. J. Elliot, *Active Control of Sound* (Academic, London, 1992).
[8]G. Canevet, "Active sound absorption in an air conditioning duct," J. Sound Vib. **58**, 333–345 (1978).
[9]P. Joseph, S. J. Elliott, and P. A. Nelson, "Near field zones of quiet," J. Sound Vib. **172**, 605–627 (1993).
[10]S. K. Lau and S. K. Tang, "Sound fields in a rectangular enclosure under active sound transmission control," J. Acoust. Soc. Am. **110**, 925–938 (2001).
[11]J. Tao, S. Wang, X. Qiu, and J. Pan, "Performance of an independent planar virtual sound barrier at the opening of a rectangular enclosure," Appl. Acoust. **105**, 215–223 (2016).
[12]A. Omoto and K. Fujiwara, "A study of an actively controlled noise barrier," J. Acoust. Soc. Am. **94**, 2173–2180 (1993).
[13]C. R. Hart and S. K. Lau, "Active noise control with linear control source and sensor arrays for a noise barrier," J. Sound Vib. **331**, 15–26 (2012).
[14]B. Kwon and Y. Park, "Interior noise control with an active window system," Appl. Acoust. **74**, 647–652 (2013).
[15]H. H. Huang, X. J. Qiu, and J. Kang, "Active noise attenuation in ventilation windows," J. Acoust. Soc. Am. **130**, 176–188 (2011).

[16]Y. G. Tong, S. K. Tang, and K. L. Tsui, "Sound transmission across a plenum window with an active noise cancellation system," Noise Control Eng. J. **64**, 423–431 (2016).
[17]S. E. Wright and B. Vuksanovic, "Active control of environmental noise," J. Sound Vib. **190**, 565–585 (1996).
[18]S. E. Wright and B. Vuksanovic, "Active control of environmental noise II: Non-compact acoustic sources," J. Sound Vib. **202**, 313–359 (1997).
[19]J. Guo, J. Pan, and C. Bao, "Actively created quiet zones by multiple control sources in free space," J. Acoust. Soc. Am. **101**, 1492–1501 (1997).
[20]D. Duhamel and P. Sergent, "Active noise control of an incoherent line source," J. Sound Vib. **212**, 141–164 (1998).
[21]J. S. Bolton, B. K. Gardner, and T. A. Beauvilain, "Sound cancellation by the use of secondary multipoles," J. Acoust. Soc. Am. **98**, 2343–2362 (1995).
[22]W. Chen, H. Pu, and X. Qiu, "A compound secondary source for active noise radiation control," Appl. Acoust. **71**, 101–106 (2010).
[23]P. L. Miller, "Room air diffusion systems–design techniques–air diffusion performance index," ASHRAE J. **19**, 37–40 (1977).
[24]L. E. Kinsler, A. R. Frey, A. B. Coppens, and J. V. Sander, *Fundamentals of Acoustics*, 4th ed. (Wiley, New York, 2000).
[25]P. A. Nelson, A. R. D. Curtis, S. J. Elliott, and A. J. Bullmore, "The active minimization of harmonic enclosed sound field. Part I: Theory," J. Sound Vib. **117**, 1–13 (1987).
[26]X. Qiu and C. H. Hansen, "Secondary acoustic source types for active noise control in free field: Monopoles or multipoles?," J. Sound Vib. **232**, 1005–1009 (2000).
[27]T. A. Beauvilain, J. S. Bolton, and B. K. Gardner, "Sound cancellation by the use of secondary multipoles: Experiments," J. Acoust. Soc. Am. **107**, 1189–1202 (2000).
[28]B. Berglund, P. Hassmén, and R. F. S. Job, "Sources and effect of low-frequency noise," J. Acoust. Soc. Am. **99**, 2985–3002 (1996).
[29]M. Mehta, J. Johnson, and J. Rocafort, *Architectural Acoustics. Principles and Design* (Prentice-Hall, New Jersey, 1999).